EVALUATION AND MODELING OF A HIGH-TEMPERATURE, HIGH-PRESSURE, HYDROGEN SEPARATION MEMBRANE FOR ENHANCED HYDROGEN PRODUCTION FROM THE WATER-GAS SHIFT REACTION

R. M. Enick, B. D. Morreale, and J. Hill

Department of Chemical and Petroleum Engineering
University of Pittsburgh
1249 Benedum Hall, Pittsburgh, PA, 15261

K. S. Rothenberger, A. V. Cugini, R. V. Siriwardane, and J. A. Poston

U.S. Department of Energy
National Energy Technology Laboratory
P.O. Box 10940, Pittsburgh, PA 15236-0940

U. Balachandran, T. H. Lee and S. E. Dorris

Energy Technology Division
Argonne National Laboratory
Argonne, IL 60439.

W. J. Graham and B. H. Howard

Parsons Project Services Incorporated
National Energy Technology Laboratory
Library, PA 15129

ABSTRACT

A novel configuration for hydrogen production from the water gas shift reaction is proposed using high temperature to enhance the rate of reaction and employing a hydrogen separation membrane for the collection of the high purity hydrogen product. Experimental high-temperature, high-pressure flux measurements have been made on a material that shows promise for such an application. Mixed oxide and metal "cermet" ion-transport disk membranes, fabricated at Argonne National Laboratory, were evaluated for hydrogen permeability on a unique high-temperature, high-pressure test unit constructed at the National Energy Technology Laboratory. Hydrogen permeation was found to be proportional to $\Delta P_{H2}^{0.5}$. At 700°C, the membrane permeability was 9.62×10^{-3} [cm^2/min][mol/lit]$^{0.5}$, or 5.63×10^{-9} [mol/m s Pa$^{0.5}$]. The membrane permeability increased to 3.31×10^{-2} [cm^2/min][mol/lit]$^{0.5}$, or 1.76×10^{-8} [mol/m s Pa$^{0.5}$] at 900°C. The membrane material was also characterized for surface changes and structural integrity using scanning electron microscopy/ X-ray microanalysis, and X-ray photoelectron spectroscopy as a function of temperature, pressure, and hydrogen exposure. Although the membrane performed well for the short periods of time employed in this study, long-term stability remains a concern. The feasibility of using this mixed-oxide ceramic

membrane to remove hydrogen from the reaction mixture was modeled for the optimization of the water-gas shift reaction. This reversible reaction is characterized by a very low equilibrium constant at elevated temperatures (>800°C); consequently CO conversion at these temperatures is typically less than 50%. In the scenario modeled, CO conversion was increased from 35% in the absence of a membrane to 79% with a membrane present, with still higher values possible if hydrogen was actively removed from the permeate side of the membrane. In the model, the effectiveness of the configuration is limited by the buildup of hydrogen partial pressure on the permeate side of the membrane. The model provided estimates of the conversion of CO attained for a specified feed, reactor size and permeate pressure.

INTRODUCTION

The demand for hydrogen is expected to rise in coming years with increases in its use both directly as a fuel and indirectly in the synthesis or upgrading of fuels required to meet increasingly demanding environmental standards. Industrial processes used to produce hydrogen, such as steam reforming of natural gas, or the gasification of heavy carbonaceous materials, generally proceed at elevated temperatures and/or pressures and produce hydrogen mixed with other gases. The recovery of hydrogen from high-temperature, high-pressure streams without the need for cooling or depressurization would enhance the efficiency and performance of systems based on such streams. Advances in the area of membrane technology may provide the basis for improved methods of hydrogen recovery and thus reduce the cost associated with hydrogen production at elevated temperature and pressure.

The water-gas shift reaction is important as a method for further enhancing the yield of hydrogen from such aforementioned industrial processes. However, the production of hydrogen via the water-gas shift reaction is favored at low temperatures. Therefore, the common approach when using the water-gas shift reaction has been to decrease the temperature of the process to favor the formation of hydrogen, and to employ a catalyst to enhance the kinetics of reaction. If the reactant gases were produced at high temperature, a loss of efficiency results upon lowering the temperature. In addition, the need for a catalyst increases costs and introduces an added degree of complexity into the reaction process.

In this paper, we will present a model of a novel configuration for hydrogen production from the water-gas shift reaction. This configuration will involve running the water-gas shift at high temperature while employing a hydrogen separation membrane for collection of the hydrogen product [Enick et al, 1999]. The high temperature will improve overall process efficiency while obviating the need for a catalyst to speed the reaction. The membrane will shift the otherwise unfavorable equilibrium towards the production of hydrogen. In addition, we will add credence to the feasibility of such a configuration by presenting experimental hydrogen flux data taken at high temperatures and pressures on small disk samples of a proton conducting ceramic-metal material. Such a material, though still in the early stages of development, has the potential to serve as a hydrogen separation membrane in high severity process environments.

The Water-Gas Shift Reaction

The water-gas-shift reaction (Eqn. 1) has been studied extensively as a basis for improving the yield of hydrogen production. In many applications, including ammonia synthesis or fuel reforming for proton exchange membrane (PEM) fuel cells, the maximum acceptable level of CO in hydrogen is in the parts per million range, therefore the water-gas shift reaction is needed.

$$CO + H_2O \Leftrightarrow CO_2 + H_2 \qquad (1)$$

There is no change in the number of moles as the reaction proceeds; therefore, the equilibrium conversion is not affected by pressure. Side reactions associated with the water-gas-shift reaction are usually not significant.

The equilibrium constant for this exothermic reaction (K, which can be expressed in terms of the concentrations of the reactants and products, Eqn. 2) decreases as temperature increases. For example, the value of K decreases from 3587 at 373 K to

0.5923 at 1273 K, as found in a published table of equilibrium values [Rostrup-Nielsen, 1984].

$$K = \frac{[CO_2][H_2]}{[CO][H_2O]} \qquad (2)$$

Therefore, conversion of CO to CO_2 (low concentrations of CO and H_2O, high concentrations of CO_2 and H_2) is favored at low temperature [Benson, 1981]. The low equilibrium conversion of CO to CO_2 at elevated temperatures is the major reason that most theoretical, experimental and industrial studies of the water-gas shift reaction are conducted at low to moderate temperatures.

Kinetics of the Water-Gas Shift Reaction

Most heterogeneous catalysis studies of the water-gas shift reaction have been conducted at temperatures less than 450^oC. Examples of commercial water-gas shift catalysts include Fe_3O_4-Cr_2O_3 and $CuZnO/Al_2O_3$ [Keiski et al., 1993]. The kinetics associated with these catalysts can be adequately described with pseudo-first order or power law kinetics [Keiski et al., 1993]. Another study of the stationary and transient kinetics of this reaction [Keiski et al., 1996] indicated that various mechanisms and kinetic expressions have been proposed for the water-gas shift reaction, and that Langmuir-Hinshelwood and power-law kinetic models are adequate. An earlier study of the water-gas shift reaction over a chromia-promoted iron oxide catalyst not only accounted for temperature and pressure, but also the catalyst age, diffusion and gas-phase composition including H_2S concentration [Singh and Saraf, 1977]. The water-gas shift reaction also occurs in some processes that do not employ catalysts. For example, the supercritical water oxidation of organic wastes (typically conducted at 400-550°C, 200-300 bar) usually does not employ a catalyst because of the rapid destruction rates that are achieved. The very high rate of the water-gas shift reaction observed in this system [Helling and Tester, 1987; Holgate et al., 1992; Rice et al., 1998] was attributed to the formation of "cages" of water about the reactants under supercritical conditions and very high water concentrations.

There is relatively little information on the kinetics of the water-gas shift reaction at elevated temperatures (>600°C). This can be primarily attributed to the diminished value of K, which would limit CO conversion to unacceptably low levels in conventional reactors. Catalysts are typically not used at elevated temperatures because of the rapid rate of the non-catalyzed reaction and catalyst instability at these extreme conditions. A study of the forward and reverse reactions of the water-gas shift reaction (Eqn. 1) was conducted at extremely high temperatures and low pressure (800-1100°C, 1 bar) [Graven and Long, 1954]. No catalyst was employed and power-law kinetic expressions were developed for the forward and reverse reactions. Despite the rapid attainment of equilibrium conversions without a catalyst, the ability to convert high temperature (800-1000° C) CO-rich combustion gases into hydrogen fuel via the water-gas shift reaction is limited by the low equilibrium conversions of CO.

Enhancing the Production of Hydrogen by Hydrogen Removal with Membranes

It has long been recognized that high levels of conversion in equilibrium-limited reactions can be achieved if one or more of the products can be extracted during the reaction. For a given value of the equilibrium constant in Eqn. 2, if the concentration of either CO_2 or H_2 is reduced the concentrations of CO and H_2O must also decrease, thereby increasing the conversion of CO. Previous investigators have established that hydrogen-permeable membranes provide a means of increasing hydrogen production in the water-gas shift reaction, steam reforming reactions, or other reversible reactions that produce hydrogen, such as the dehydrogenation of ethylbenzene or cyclohexane. The use of catalytic or inert hydrogen permeable membranes in a reactor would result in the removal of hydrogen from the reaction mixture, leading to an increase in feedstock conversion in the equilibrium-limited reactions yielding hydrogen as a product [Armor, 1995; Sun and Khang, 1988; Liu et al., 1990; Barbieri and DiMaio 1997a,b; Uemiya et al., 1991a,b; Tsotsis et al., 1992; Itoh et al., 1993; Adris et al., 1994; Netherlands Energy Research Foundation, 1995; Basile et al., 1996a,b; Mardilovich et al., 1998]. In this study, only the water-gas shift reaction was modeled.

Membrane Characterization

Currently, several research organizations are engaged in the development of hydrogen transport membranes or their precursor materials [Balachandran et al., 1998; Fain and Roettger 1993; Peachey et al., 1999; Mardilovich; et al., 1998]. Membrane materials range from organic polymers to metals to ceramics. Non-porous (high density) ceramic membranes are particularly desirable because they can be made exclusively selective to hydrogen and are durable enough to withstand high temperature, high pressure conditions that would be encountered in the proposed commercial application [Balachandran et al., 1998]. Practical application of these membranes would likely employ a high inlet pressure coupled with reduced pressure on the outlet side of the membrane to enhance the flux. Hydrogen flux through these membranes is expected to be optimal in the range of 700-900EC and increase with an increasing hydrogen partial pressure gradient across the membrane. The proton-conducting ceramic membranes that were used in this study were developed at Argonne National Laboratory (ANL). These dense ceramic membranes were fabricated from mixed protonic /electronic conductors and had previously been tested at ANL under ambient pressures. Hydrogen selectivity was very high because the membranes do not have interconnected pores so the only species that pass through the membranes are those that participate in ionic conduction, such as hydrogen. [Balachandran et al., 1998]. These membranes had not been previously tested at elevated pressures or over a wide range of hydrogen concentrations.

The goal of this study was the characterization of the ANL ion-transport membrane at elevated temperatures (700-900°C) and pressures (ΔP_t<250 psi) that were relevant to the water-gas shift reaction concept. Hydrogen permeability was evaluated using steady state measurements of hydrogen flux through the membrane. Characterization of surface changes and structural integrity were performed using scanning electron microscopy/ X-ray microanalysis (SEM/EDS), X-ray photoelectron spectroscopy (XPS) and atomic force microscopy (AFM), as a function of temperature and hydrogen exposure. Steady-state hydrogen flux measurements over the 700-900°C range at hydrogen partial pressure differences up to 250 psi were used to characterize hydrogen permeability. The expression derived for the hydrogen permeability of the membrane was then included in the water-gas shift membrane-reactor model.

EXPERIMENTAL METHODS

Cermet membranes, consisting of a metal oxide base mixed with a metal, were fabricated by a process developed at ANL. The membranes used in this study were of composition "ANL-1", with an oxide of composition $BaCe_{0.80}Y_{0.20}O_3$ (BCY) with nickel as the added metal. The BCY ceramic base was prepared by mixing appropriate amounts of $BaCO_3$, CeO_2 and Y_2O_3, then calcining the mixture at 1000°C for 12 hours in air. The powder was then ball-milled and calcined again at 1200°C for 10 hours in air. After obtaining phase-pure powder (as determined by X-ray diffraction), the BCY powder was mixed with 40 vol% metallic nickel powder to increase its electronic conductivity. The powder mixture was then uniaxially pressed and sintered for 5 hours at 1400-1450°C in an atmosphere of 4% hydrogen /96% argon. The disk membranes were typically 0.04 - 0.06 in (1.0 - 1.5 mm) in thickness.

Membranes for pressure and flux testing were mounted, using a brazing process developed at ANL, within four inch long, 0.75 in. O.D., heavy-wall, Iconel 600 tubing which had been machined to form a small seat to accommodate the membrane. Typically, the membrane diameter was 0.69 in. (17.5 mm.). Unmounted membranes of the same composition, as well as membranes of varying Ni content, were also available for characterization studies. Because the pressure tested membranes had to be pre-mounted, the before-and-after characterization studies refer to membranes of the same composition and fabrication, but not the same physical membranes.

Membrane pressure and flux testing was performed using the Hydrogen Membrane Testing (HMT) unit which was constructed in the Hydrogen Technology Research (HTR) facility at the National Energy Technology Laboratory (NETL). The facility made use of the high pressure hydrogen handling infrastructure previously put in place for the study of high pressure hydrogenation reactions [Cugini et al., 1994]. For membrane testing, the unit has an operating range from ambient temperature to 900EC and ambient pressure to

450 psig. The Inconel 600 tubing containing the pre-mounted membrane from ANL was welded to an additional length of 0.75 in. O.D. Inconel 600 tubing. The membrane was hung in an inverted configuration and attached to a second piece of 0.75 in. OD Inconel 600 tubing by means of an Inconel 600 sleeve. A ceramic fiber heater was positioned around the sleeve for heating the membrane. The entire assembly was suspended within a 2-gallon stainless steel autoclave that was continuously purged with nitrogen gas. A simplified schematic of the test assembly is shown in Figure 1.

Both cold and hot inert gas pressure tests were performed on samples of brazed cermet membranes in advance of hydrogen flux measurements in order to ascertain the integrity of the Inconel 600-to-cermet seal under high temperature and pressure conditions. The procedure used in these tests has been described elsewhere [Rothenberger et al., 1999].

Hydrogen flux measurements were performed on three separate ANL-1 cermet membranes. Three different test gases - 100% hydrogen, a 50% hydrogen /50% nitrogen mixture, and a 10% hydrogen /90% nitrogen mixture - were introduced in a flowing mode to the retentate (feed) side of the membrane. The flow rate, typically 190 ml/min STP, was sufficient such that the overall composition of the retentate side did not change significantly due to hydrogen permeation. Operating temperatures ranged from 700-900EC as measured by a thermocouple positioned on the permeate side of the membrane, approximately 0.25 in. above the membrane surface (Figure 1). Test gas pressures were stepped both up and down in 10-50 psi increments between atmospheric pressure and 250 psig. Pressure conditions were held from one to four hours, depending on the magnitude of the step from the previous reading, and whether the flux data had reached a constant value. Usually, the flux data reached a constant value within 10-20 minutes. The permeate-side of the membrane was swept with argon, and the effluent was monitored with a gas chromatograph (GC) for hydrogen concentration using an argon carrier gas. GC measurements were recorded every 10 minutes during flux testing. The argon sweep rate was maintained at 85 ml/min STP, resulting in hydrogen concentrations in the sweep gas in the range of 0.01 to 3.0 percent. Nitrogen detected by GC was indicative of a membrane leak. Although the experiments were allowed to continue with a leaking membrane, only data taken before the detection of a leak was used in the membrane permeance evaluation for this paper.

Because the Inconel 600 metal alloy used as a mounting material for the membrane itself becomes permeable to hydrogen under the test conditions, a separate experiment, configured in a similar manner, was performed to determine the permeance of the Inconel 600.

X-ray photoelectron spectroscopy (XPS) spectra were recorded with a Physical Electronics model 548 XPS system. The binding energies were referenced to the C(1s) level at 284.6 eV for adventitious carbon. XPS data were obtained at various temperatures ranging from room temperature to $650^{o}C$. X-ray microanalysis was performed at room temperature and $575^{o}C$ using a JOEL 840-A scanning electron microscope equipped with a Noran Instruments Micro-Z energy dispersive spectrometer, which was interfaced to a Noran Instruments Voyager-4 computer. Detector resolution, as referenced to the manganese $K\alpha$ spectra line, was 148 eV.

Data obtained at NETL for hydrogen flux through the ANL-1 dense ceramic membranes were correlated to yield a flux expression. The flux of hydrogen through these membranes, R_{H2}, was found to be proportional to the permeability of the membrane, k_{H2}, and was assumed to be inversely proportional to the membrane thickness, t_m, as is typical with other hydrogen permeable membrane materials. The driving force for the hydrogen flux was related to the hydrogen partial pressure, P_{H2}, or molar concentration of hydrogen, C_{H2}, raised to the exponent n (the units of k are dependent upon the value of n), with the units of R'_{H2} (mol/s), R_{H2} (mol/s), A_m (m^2), t_m (m), C_{H2} (mol/L), and P_{H2} (Pa).

$$R'_{H2} = \frac{A_m k'_{H2} \left(C_{H2,retentate}{}^n - C_{H2,permeate}{}^n \right)}{t_m} * 1.67 x 10^{-3} \tag{3}$$

$$R_{H2} = \frac{A_m k_{H2} \left(P_{H2,retentate}{}^n - P_{H2,permeate}{}^n \right)}{t_m} \tag{4}$$

Now, flux will be equivalent regardless of the form of the driving force, therefore

$$R'_{H2} = R_{H2} \tag{5}$$

If transport through a membrane involving both surface reaction (dissociation) and diffusion was limited by surface reactions, then n = 1. If transport was diffusion-limited, then n = 0.5. Intermediate values of n (0.5<n<1) have also been reported [Uemiya et al., 1991a; deRossett 1960; Hurlbert and Konecny, 1961]. In this study, the flux of hydrogen through the proton transport membranes was modeled with the same form of the equations used to model diffusion membranes, Eqns. 3 and 4. Values of k'_{H2} and n were determined from Eqn. 3. The concentration of hydrogen on the permeate-side was insignificant relative to the concentration on the retentate-side. Therefore $C_{H2,permeate}$ was equated to zero. Thus, taking the logarithm of both sides of Eqn. 3 yields,

$$\log R_{H2} = n \log C_{H2,retentate} + \log(A_m k'_{H2} / t_m) \tag{6}$$

Therefore, a log-log plot of hydrogen permeation through the membrane, R_{H2} [mol/min] versus retentate hydrogen concentration, $C_{H2,permeate}$ [mol/cm^3], yielded a straight line of slope n. The value of k'_{H2} was determined from the intercept because both membrane area, A_m, and membrane thickness, t_m, were known. Membrane areas were in the 1.25-1.36 cm^2 range, depending on the specific to wall thickness used for membrane mounting, and membrane thickness was in the 1.1-1.3 mm range.

Subsequent studies of these proton-transport membranes will be conducted over a wide range of hydrogen partial pressures on the permeate-side. This will allow assessment of whether the driving force for hydrogen permeance is more accurately represented as the natural logarithm of the ratio of the hydrogen partial pressures on the retentate- and permeate-sides, as observed in ion-transport oxygen membranes.

RESULTS AND DISCUSSION

Membrane Characterization

The cold and hot inert gas pressure tests on the sealed ANL-1 membranes are described elsewhere [Rothenberger et al., 1999]. The results indicated that the membrane to substrate seal was gas tight to 400 psig at temperatures up to 800^{N}C, at least for short periods of time. However, a small leak developed at a temperature of 800^{N}C and a pressure of 450 psig. After cool down, visual inspection of the membrane revealed a white powdery coating on and around the membrane. Small areas of green discoloration were observed around the surface of the normally gray membrane. Some of the brazing material appeared to have migrated from around the edge of the membrane toward the center, moving a distance of approximately 0.5 mm. Migration of the braze material had previously been observed during hot ambient temperature flux testing at ANL. Visual inspection under an optical microscope revealed cracks in the membrane surface along the perimeter of the disk, as well as cracks in the brazing material itself. At this time, it is not known whether the failure was strictly a pressure effect, or if the elevated temperature and possible migration of some of the brazing material was involved. Because the hydrogen membrane testing unit was still under construction at the time of the pressure tests, the permeate side of the membrane was exposed to atmospheric oxygen during the inert gas pressure tests. The membrane material is also permeable to oxygen at high temperature, and the presence of what is probably oxide contamination around the membrane after the hot pressure test indicated that some degradation of the membrane and/or sealing materials may have occurred as a result of air exposure. Following the inert gas pressure tests, it was decided to limit the pressure drop across the membrane during flux testing to 250 psi.

Hydrogen flux testing of the ANL-1 cermet membranes was conducted on the HMT unit. Data from these runs is plotted in Figure 2.

The unit behaved as expected, with increased hydrogen flux observed as a function of increased hydrogen partial pressure and increased membrane temperature from 700°C to 900°C. Operational difficulties were encountered in maintaining feed gas flow rate at pressures approaching 250 psig, resulting in drifting or poorer quality data at those values. A small systematic bias was also observed resulting in slightly (approximately 5%) higher flux readings detected when stepping down to a given pressure than when stepping up to the same pressure. However, no attempt was made to select or discard

individual data points. All data points taken during a given test period were used in the assessment of membrane performance. For the three membranes that were tested, leakage was detected after approximately 70, 50, and 20 hours of use, respectively. No data taken after the detection of any leak was used in the permeance analysis. Physical and microscopic examination of the membranes after testing revealed that the leak was generally located in the area of the ceramic to metal seal, rather than in the body of the membrane itself.

Hydrogen flux measurements made on the Inconel 600 mounting material revealed permeance values between 1 and 10 percent of those measured for the cermet membrane mounted in the Inconel 600. The measured hydrogen flux for the mounted membrane includes a flux contribution from the Inconel 600 holder. Unfortunately, it was impossible to make a direct measurement of hydrogen bypassing the membrane during a flux test. But in order to bypass the membrane, hydrogen permeating through the Inconel 600 mount had to diffuse first into the very tight space between the Inconel 600 sleeve and the mounting tube. Although hydrogen gas is certainly capable of this, the amount of hydrogen diffusing into the sweep zone via this route would have been limited by mass transport considerations, and thus, smaller than the amount experimentally measured for Inconel 600. Therefore, it was decided not to make any adjustments or corrections to the membrane permeance data at this time.

SEM microanalysis was conducted to determine the changes in morphology, elemental distribution and composition that occur to a fresh ANL-1 membrane upon heating. A photomicrograph of a fresh membrane is shown in Figure 3a. No major morphological changes were observed after heating the membrane from room temperature to 575°C under an inert atmosphere. Elemental distribution was uniform and remained uniform following heating and hydrogen exposures at 575°C. SEM analysis of a 40% Ni /BCY membrane after flux testing revealed quite different results. Morphology more closely resembled the membrane samples with much lower Ni contents. X-ray microanalysis confirmed a lower Ni content in the near surface region as compared to the fresh membrane. A photomicrograph of a membrane after flux testing is shown in Figure 3b.

XPS was utilized to determine the elemental composition and oxidation states of elements in approximately the top 50 Δ of the surface of a fresh membrane during heating. At room temperature, surface nickel was oxidized and the intensity of the nickel peak was low. When the membrane was heated to 650EC under vacuum, the intensity of the nickel peak increased substantially and the nickel was reduced to the metallic state. The ratios of Ni/Ba, Ni/Ce and Ni/Y at the surface increased when the temperature was increased, as shown in Table 1, but they decreased again when the membrane was cooled back to room temperature. Thus, the nickel "migrated" or otherwise became more apparent at the surface and preferentially resided there relative to the other elements at higher temperature.

XPS analysis was also performed on the membrane following the flux test. At room temperature, only Ba was detected on the surface of the tested membrane. Ni, Ce, and Y could not be detected as shown in Table 1. When the sample was heated to 650EC under vacuum, it was possible to detect a small quantity of Ni and Y, but no Ce (Table 1). Ba had the highest concentration at the surface both at room temperature and 650EC (Table 1). The relative concentration of Ni at the surface was significantly lower on the tested membrane than on the fresh membrane. The small amount of Ni observed at 650EC on the tested membrane did not appear to be in the metallic state. The XPS results indicated that there was a permanent loss of Ni from the surface region over the course of flux testing.

Table 1: Relative elemental composition at the surface of the fresh membrane and after H_2 flux testing.

Condition	Ni / Ba	Y / Ba	Ce / Ba
Fresh at 25 ^{o}C	0.17	0.75	0.28
Fresh at 650°C	0.80	0.38	0.22
After H_2 test at 25°C	0	0	0
After H_2 test at 650°C	0.02	0.04	0

Although the membrane and sealing methodology are impermeable to nitrogen and helium and are capable of withstanding high temperatures and high-pressure differentials for short periods of time, the seal appears to degrade over a 50-100 h time period at elevated temperature under any pressure. In addition, surface characterization results indicate that irreversible changes occur to the membrane itself. These results call into question the membrane seal applicability for long-term use in harsh operating environments and provide a challenge for future improvements in the technology.

Hydrogen Permeance

Values of k_{H2} and n at elevated temperatures and pressures were determined from hydrogen flux data. The log-log representation of this data (Eqn. 6) in terms of hydrogen partial pressure is illustrated in Figure 2. The n values were 0.51, 0.53 and 0.55 at 700, 800 and 900°C, respectively. This value of approximately 0.5 is similar to the values reported for diffusion membranes such as palladium [Armor, 1995]. The temperature-dependent k_{H2} value was determined from the intercept of each set of data. The results were then fit to an Arrenhius relation (Eqn. 7),

$$k'_{H2} = k_o \exp\left[\frac{-E}{8.314T}\right] \tag{7}$$

with a membrane activation energy value, E, of 58,600 J/mol, temperature in Kelvin and a pre-exponential constant value, k_o, of 13.4 [cm^2/min][mol/liter]$^{0.5}$. For example, at 700°C (973 K), the permeability of the membrane, k'_{H2}, was 9.62x10^{-3} [cm^2/min][mol/liter]$^{0.5}$, which corresponded to a k_{H2} value of 5.63x10^{-9} [mol/(m s Pa$^{0.5}$)]. The membrane permeability increased to 3.31x10^{-2} [cm^2/min][mol/lit]$^{0.5}$, or 1.76x10^{-8} [mol/(m s Pa$^{0.5}$)] at 900°C. To facilitate comparison of hydrogen permeability of the ANL-1 proton conducting membrane and metal membrane permeability [Buxbaum and Marker, 1993], it is convenient to express the permeability with units of k_{H2} [mol/(m s Pa$^{0.5}$)]. Conversion between k'_{H2} and k_{H2} is provided below (Eqn. 8), with temperature in Kelvin.

$$k_{H2}\frac{mol}{m\ s\ Pa^{0.5}} = 1.828\times10^{-5}\frac{1}{T^{0.5}}k'_{H2}\frac{cm^2}{min}\sqrt{mol/l} \tag{8}$$

At 700°C, the permeability of palladium is approximately 3.0 x10^{-8} [mol/(m s Pa$^{0.5}$)] and the permeability of iron is 5.0x10^{-10} [mol/(m s Pa$^{0.5}$)] [Buxbaum and Marker, 1993]. Figure 4 illustrates the hydrogen permeability of palladium, iron and the proton conducting ceramic material as a function of inverse temperature. The driving force for hydrogen flux in each membrane material is $\Delta P^{0.5}$.

Modeling

Membrane reactor models of various configurations, complexity, and ranges of applicability have been previously reported [Sun and Khang, 1988; Itoh and Govind, 1989; Liu et al., 1990]. Several previous investigators have presented water-gas shift membrane reactor models. A model of the iron-chromium oxide catalyzed water-gas shift reaction at 673 K in a cylindrical, palladium membrane reactor was developed to demonstrate enhanced CO conversion [Uemiya et al., 1991a]. A packed bed catalytic membrane reactor model was used to get good agreement with experimental data by varying a single parameter, the thickness of the permselective membrane layer [Tsotsis et al., 1992]. A simple model for the water-gas shift membrane reactor was developed that assumed the reaction kinetics were so fast that equilibrium was established along the entire reactor length [Damle et al., 1994]. An ideal flow model was derived for an isothermal, cylindrical, catalyzed, water-gas shift, membrane reactor operating at temperatures up to $400^{o}C$ [Netherlands Energy Research Foundation, 1995]. The same authors also used computational flow dynamics software to model the same system under either isothermal or adiabatic conditions which accounted for two-dimensional flow and axial and radial dispersion [Netherlands Energy Research Foundation, 1995].

Unlike these previous models, the objective of this study is to model a non-catalyzed, high temperature, proton-conducting membrane reactor that incorporates reaction kinetics. Therefore, the high temperature, high pressure hydrogen permeance of the ANL-1 proton-conducting membranes was integrated into a water-gas shift membrane reactor model in this study, along with previously published high temperature, non-catalyzed reaction rate results [Graven and Long, 1954]. The configuration of the reactor was similar to the multiple, parallel tubular membranes envisioned for commercial applications [Parsons, 1998]. The model was used to estimate the permeate pressure and/or surface area of the membrane required to achieve a desired level of CO conversion or hydrogen recovery. Alternately, it was used to provide estimates of the hydrogen permeability the membrane must exhibit to attain a specified CO conversion or H_2 recovery in a reactor with a specified membrane area.

The basis of the model is a tubular membrane located within a coaxial cylindrical shell. The feed gases are introduced on the shell-side (reaction-side, annular-side, retentate-side, raffinate-side) of the reactor. Hydrogen permeates the membrane, and the hydrogen permeate product can be obtained from the tube-side. A schematic of the modeled membrane reactor is shown in Figure 5. As the reaction gases proceed down the length of the reactor, hydrogen will continue to permeate the membrane if the partial pressure of hydrogen on the reaction side exceeds the permeate hydrogen partial pressure, increasing the conversion of the CO. The high-pressure CO_2-rich retentate exits the reactor on the shell-side, and a low-pressure, high-purity hydrogen permeate is recovered from the tube-side. Use of a sweep gas is not desirable to avoid subsequent separations of hydrogen from sweep gas. Absence of a sweep gas will result in a substantial pressure drop across the wall of the membrane.

The design equations for a tubular plug flow reactor are based on ordinary differential mass balances for each component [Fogler, 1992; Netherlands Energy Research Foundation, 1995]. The model predicts the performance of the reactor under steady-state isothermal conditions. The reactants and products are assumed to behave as ideal gases. The pressure drop along the length of the reactor is assumed to be negligible for both the retentate-side and the permeate-side of the reactor. Published correlations for the equilibrium constant (K) [Benson, 1981; Netherlands Energy Research Foundation, 1995; Singh and Saraf, 1977] can be used for pseudo-first order or power-law kinetic expressions. Reaction kinetics are described by non-catalytic, high temperature 800-$1100^{o}C$ expressions [Graven and Long, 1954]. The results of their model are summarized by reaction rate expressions for the forward and reverse reactions.

$$-\frac{d[H_2O]}{dt}\frac{mol}{min\ liter}=\frac{60(9.5\times10^{10}\exp{(-57000/1.987T)}[H_2]^{0.5}[CO_2])}{(1+3.6\times10^3[CO])} \qquad (9)$$

$$-\frac{d[CO_2]}{dt}\frac{mol}{min\ liter}=\frac{60(5.0\times10^{12}\exp{(-67300/1.987T)}[CO]^{0.5}[H_2O])}{(1+1.2\times10^4[H_2])^{0.5}} \qquad (10)$$

As Graven and Long noted, these expressions were based on conditions removed from equilibrium. If the forward and reverse reaction rates are equated to determine the equilibrium constant, there will be disagreement between the result and well-established correlations for the equilibrium constant. Therefore, we modified their model in the following manner to yield the correct equilibrium constant.

$$-\frac{d[CO_2]}{dt}\frac{mol}{min \cdot liter} = \frac{60(5.0\times10^{12}\exp(-67300/1.987T)[CO]^{0.5}[H_2O])}{(1+1.2\times10^4[H_2])^{0.5}}(1-\boldsymbol{b}) \qquad (11)$$

$$\boldsymbol{b} = \frac{[CO_2][H_2]}{[CO][H_2O][K_{eq}]} \qquad (12)$$

A recent correlation for the equilibrium constant was used [Netherlands Energy Research Foundation, 1995].

$$K_{eq} = \exp\left\{-4.33 + \frac{4577.8}{T(\text{K})}\right\} \qquad (13)$$

The conditions listed in Table 2 are associated with a conceptual coal processing plant for producing hydrogen while recovering carbon dioxide [Parsons 1999]. The highest possible conversion of CO for the water-gas shift reaction in the absence of a membrane is 35%. The single tube reactor, Figure 5, can represent many parallel reactor membrane tubes within a large reactor shell.

Table 2: Model conditions and assumptions used in the single tube example.

Catalyst	No catalyst used at this high temperature
Mode of Operation	Isothermal
Temperature	900^oC; 1173 K
Reaction-Side	Annular-side, Shell-side
Pressure on reaction-side	27 atm
Pressure on tube-side	1.0 atm
Reactor length	700 cm
Reactor diameter (for each tube)	5.0 cm
Tube-side sweep gas	None
Membrane	Proton Transport
Membrane diameter	2.0 cm
Permeable gases	Hydrogen Only
Membrane thickness	0.1 cm (1 mm)
Membrane driving force	$C_{H2,retentate}^{0.5} - C_{H2,permeate}^{0.5}$
Membrane permeability	0.033 [cm^2/min][mol/liter]$^{0.5}$ (from Eq. 7)
CO inlet flow rate	0.080 gmol/min
Steam inlet flow rate	0.088 gmol/min
Hydrogen inlet flow rate	0.040 gmol/min
Reaction kinetics	Modified Graven and Long Model

The membrane reactor concentration profiles and molar flow rate profiles are illustrated in Figures 6 and 7, respectively. As the CO and H_2O enter, the CO concentration in the annulus is greater than the equilibrium concentration and the reaction proceeds rapidly. Hydrogen permeation also initiates. The reaction-side molar flow rate of hydrogen increases initially because the rate of hydrogen generation exceeds the permeation rate. The equilibrium conversion is attained 50 cm down the length of the reactor, but the conversion of CO continues as hydrogen permeates the membrane. In the middle portions of the reactor, more hydrogen is permeating through the membrane than is being generated by the water-gas shift reaction, as a result the hydrogen concentration of the retentate decreases. Near the end of the reactor, the hydrogen concentration in the permeate and retentate approach the same value, and further conversion of CO cannot be achieved because hydrogen permeation ceases and the CO concentration is at its equilibrium value. This reactor achieved a 78.7% conversion of CO.

Significant increases in equilibrium conversion beyond 78.7% can be attained in this example only if the partial pressure of hydrogen in the permeate region is reduced. This can be accomplished by operating the permeate-side of the reactor under partial vacuum or by employing a sweep gas that can be readily separated from the hydrogen in a subsequent processing step. For example, if superheated steam is used as a sweep gas, the permeate product could be cooled, condensing the water and yielding high purity hydrogen. Figure 8 illustrates the effect of hydrogen permeate partial pressure on the conversion of CO in this reactor.

CONCLUSIONS

A model of a novel configuration for hydrogen production from the water-gas shift reaction has been demonstrated. The model employs a hydrogen separation membrane for collection of the hydrogen product and high temperature for enhancing the rate of reaction. Experimental high-temperature, high-pressure flux measurements have been made on a novel material that might be suitable in such an application.

The ANL-1 cermet material tested exhibits many positive qualities for use as a hydrogen separation membrane in high-temperature, high-pressure applications. It exhibits very high selectivity, reasonable permeability, and is quite robust, being able to tolerate temperatures up to 900°C and pressure drops up to 400 psi. However, membrane-to-substrate seal methodology is an area for improvement, as seal integrity for membranes tested both at NETL and ANL was limited to durations of less than 100 hours. Both visual and spectroscopic investigation of membranes after testing suggested that the sealing and membrane materials may have reacted. A possible way to mitigate this situation might be to remove the seal from the hot zone.

Membrane surface characterization and analysis indicated that significant elemental and oxidative changes occurred on the membrane surface upon heating, and again after flux testing. In particular, XPS indicated that metallic Ni "migrated" or otherwise appeared at the surface of a fresh membrane at elevated temperature. Some of this nickel could have migrated from the braze material. After testing, both XPS and SEM/EDS indicated a loss of Ni in the surface and near surface regions. Therefore, transport of hydrogen through the membrane over an approximately 50-hour period appeared to result in permanent changes to the membrane. The effect of such changes, both temporary and permanent, on membrane strength, interactions between the membrane and sealing material, and/or the ability of the membrane to transport hydrogen are not yet understood. However, material stability would certainly be a desired quality for any commercial or industrial applications. These results provide goals for future improvements in the technology.

High-temperature, high-pressure hydrogen flux measurements for these membranes indicated that the permeation of hydrogen was proportional to the square root of hydrogen concentration or partial pressure. The permeability of this proton-conducting membrane was found to be 9.62×10^{-3} [cm^2/min][mol/lit]$^{0.5}$, intermediate to that of palladium and iron, at 700°C. The permeability increased with temperature at 800 and 900°C. The temperature-dependence of the membrane's hydrogen permeability was expressed in an Arrhenius relationship.

A model of a tubular, plug flow membrane reactor was developed for evaluating the effect of hydrogen permeable membranes on the conversion of CO in the water-gas shift reaction. The model has been developed for very high temperature systems (>800°C) that

14

do not employ a catalyst. Under these conditions, the presence of a membrane increased conversion of CO from 35% to 79%, with still higher values possible if hydrogen was actively removed from the permeate side of the membrane. The model can incorporate hydrogen permeation/diffusion models that are appropriate for novel high-temperature, high-pressure membranes currently being developed. This tool can be used to assess the levels of CO conversion, H_2 purity and recovery, and CO_2-rich retentate flow rate and recovery that can be realized in a reactor of specified geometry if proton-conducting membranes are incorporated. The model can also be used to provide "targets" for the hydrogen permeability required to make this technology economically feasible.

ACKNOWLEDGEMENTS AND DISCLAIMER

REFERENCES

Adris, A.; Lim, C.; Grace, J.; The Fluidized Bed Membrane Reactor System: A Pilot-Scale Experimental Study; Chemical Engineering Science 49, No. 24B (1994) 5833-5843.

Armor, J.; Membrane Catalysis: Where Is It Now, What Needs to be Done?; Catalysis Today 25 (1995) 199-207.

Balachandran, U.; Guan, J.; Dorris, S. E.; Liu, M.; Development of Proton-Conducting Membranes for Separating hydrogen from Gas Mixtures; extended abstract of presentation at the AIChE 1998 Spring Meeting, New Orleans, LA, March 8-12, 1998.

Barbieri, G.; DiMaio, F.; Simulation of the Methane Steam reforming Process in a Catalytic Pd-Membrane Reactor; Ind. Eng. Chem. Res. 36 (1997) 2121-2127.

Barbieri, G,; Violante, V.; DiMaio, F.; Criscuoli, A.; Drioli, E.; Methane Steam reforming Analysis in a Palladium-Based Catalytic Membrane Reactor; Ind. Eng. Chem. Res. 36 (1997) 3369-3374.

Basile, A.;Criscuoli, A.; Santella, F.; Drioli, E.; Membrane Reactor for Water Gas Shift Reaction; Gas Separation and Purification 10(4) (1996a) 243-254.

Basile, A.; Drioli, E.; Santella, F.,; Violante, V.; Capannelli, G,; A Study on Catalytic Membrane Reactors for Water Gas Shift Reaction; Gas Separation & Purification 10(1) (1996b) 53-61.

Benson, H. E.; Processing of Gasification Products; Ch. 25 in Chemistry of Coal Utilization, Elliot, M., ed.; John Wiley and Sons; New York, NY, 1981.

Buxbaum, R.E.; Marker, T.L.; J; Hydrogen Transport Through Non-Porous Membranes of Palladium-Coated Niobium, Tantalum, and Vanadium; . Membr. Sci. 85 (1993) 29-38.

Cugini, A.; Krastman, D.; Lett, R.; Balsone, G.; Development of a Dispersed Iron catalysis for First Stage Coal Liquefaction; Catalysis Today 19 (1994) 395-408.

Damle, A.S.; Gangwal, S.K.; Venkataraman, V.K.; A Simple Model for a Water Gas Shift Membrane Reactor; Gas Separation & Purification 8, No. 2 (1994) 101-106.

DeRossett, A.J.; Diffusion of Hydrogen Through Palladium Membranes; Ind. Eng. Chem. 52(6) (1960) 525-528.

Enick, R.M.; Hill, J.; Cugini, A.V., Rothenberger, K.S.; McIlvried, H.G.; "A Model of a High Temperature, High Pressure Water-Gas Shift Tubular Membrane Reactor", Am. Chem. Soc., Fuel Chem. Div., Prepr. Pap., 44(4), (1999) 919-923.

Fain, D. E.; Roettger, G. E.; Coal Gas Cleaning and Purification with Inorganic Membranes; Trans. of the ASME Journal of Engineering for Gas Turbines and Power, 115 (July 1993) 628-633.

Fogler, H. S.; Elements of Chemical Reaction Engineering, Second Edition; Prentice Hall, Englewood Cliffs, NJ (1992).

Graven, W. M.; Long, F. J.; Kinetics and Mechanisms of the Two Opposing Reactions of the Equilibrium $CO + H_2O = CO_2 + H_2$; J. Amer. Chem. Soc. 76 (1954) 2602.

Helling, R.K.; Tester, J.W.; Oxidation Kinetics of Carbon Monoxide in Supercritical Water; Energy and Fuels, 1 (1987) 417-423.

Holgate, H.R.; Webley, P.A.; Tester, J.W.; CO in Supercritical Water: The Effects of Heat Transfer and the Water-Gas Shift Reaction on Observed Kinetics; Energy & Fuels, 6 (1992) 586-597.

Hurlbert, R.C.; Konecny, J.O.; Diffusion of Hydrogen through Palladium; J. of Chem. Phys. 34(2) (1961) 655-658.

Itoh, N.; Govind, R.; Development of a Novel Oxidative Palladium Membrane Reactor; AIChE Symposium Series 268, Govind and Itoh, eds.; New York, NY 1989.

Itoh, N.; Xu, W.; Sathe, A.; Capability of Permeate Hydrogen through Palladium-Based Membranes for Acetylene Hydrogenation; Ind. Eng. Chem. Res. 32 (1993) 2614-2619.

Keiski, R.I.; Desponds, O.; Chang, Y.; Somorjai, G.A.; Kinetics of the Water-Gas Shift Reaction Over Several Alkane Activation and Water-Gas Shift Catalysts; Applied Catalysis A: General, 101 (1993) 317-338.

Keiski, R.; Salmi, T.; Niemisto, P.; Ainassaari, J.; Pohjola, V.J.; Stationary and Transient Kinetics of the High Temperature Water-Gas Shift Reaction; Applied Catalysis A: General, 137 (1996) 349-370.

Liu, Y.; Dixon, A.; Ma, Y.; Moser, W.; Permeation of Ethylbenzene and Hydrogen Through Untreated and Catalytically Treated Alumina Membranes; Separation Science and Technology 25 (1990) 1511-1521.

Mardilovich, P.; She, Y.; Ma, Y.; Rei, M.; Defect-Free Palladium Membranes on Porous Stainless Steel Support; AIChEJ 44(2) (1998) 310-322.

Netherlands Energy Research Foundation ; Combined Cycle Project – IGCC with CO_2 Removal Project Area – An Attractive Option for CO_2 Control in IGCC Systems: Water Gas Shift with Integrated Hydrogen/Carbon Dioxide Separation (WIHYS) Process – Phase 1 Proof of Principle; Alderliesten, P. T. and Bracht, M., eds.; Contract JOU2-CT92-0158, Final Report (1995).

Parsons Infrastructure and Technology Group; Decarbonized Fuel Plants Utilizing Inorganic Membranes for Hydrogen Separation; presented at the 12th Annual Conference of Fossil Energy Materials, May 12-14, 1998, Knoxville, Tennessee.

Parsons Infrastructure and Technology Group; Decarbonized Fuel Plants for Vision 21 Applications, WYODAK Coal Substitution; DOE/FETC Report, April 13, 1999.

Peachey, N. M.; Snow, R. C.; Dye, R. C.; Composite Pd/Ta Metal Membranes for Hydrogen Separation; Journal of Membrane Sciences (in press).

Rice, S.F., Steeper, R. R.; Aiken, J. D.; Water Density Effects on Homogeneous Water-Gas Shift Reaction Kinetics; J. Phys. Chem. A, 102(16) (1998), 2673-2678.

Rostrup-Nielsen, J.R.; Catalytic Steam Reforming; Chapter 1 of Catalysis Science and Technology, Vol. 5; Anderson, J. and Boudart, M., eds; Springer-Verlag (1984), 1-118.

Rothenberger, K.S.; Cugini, A.V.; Siriwardane, R.V.; Martello, D.V.; Poston, J.A.; Fisher, E.P.; Graham, W.J.; Balachandran, U.; Dorris, S.E.; "Performance Testing of Hydrogen Transport Membranes at Elevated Temperatures and Pressures", Am. Chem. Soc., Fuel Chem. Div., Prepr. Pap., 44(4), (1999). 914-918.

Singh, C.P.; Saraf, D.N.; Simulation of High-Temperature Water-Gas Shift Reactors; Ind. Eng. Chem. Process Des. Dev. 16(3) (1977).

Sun, Y.; Khang, S.; "Catalytic Membrane for Simultaneous Chemical Reaction and Separation Applied to a Dehydrogenation Reaction," Ind. Eng. Chem. Res. 27 (1988) 1136-1142.

Tsotsis, A.; Champagnie, A.; Vasileiadis, S.; Ziaka, Z.; Minet, R.; Packed Bed Catalytic Reactors; Chemical Engineering Science 47(9) (1992) 2903-2908.

Uemiya, S.; Sato, N.; Ando, H.; Kikuchi, E.; The Water Gas Shift Reaction Assisted by a Palladium Membrane Reactor; Ind. Eng. Chem. Res. 30 (1991a) 585-589.

Uemiya, S.; Sato, N.; Ando, H.; Matsuda, K.; Kikuchi, E.; Steam Reforming of methane in a Hydrogen Permeable Membrane Reactor; Applied Catalysis 67 (1991b) 223-230.
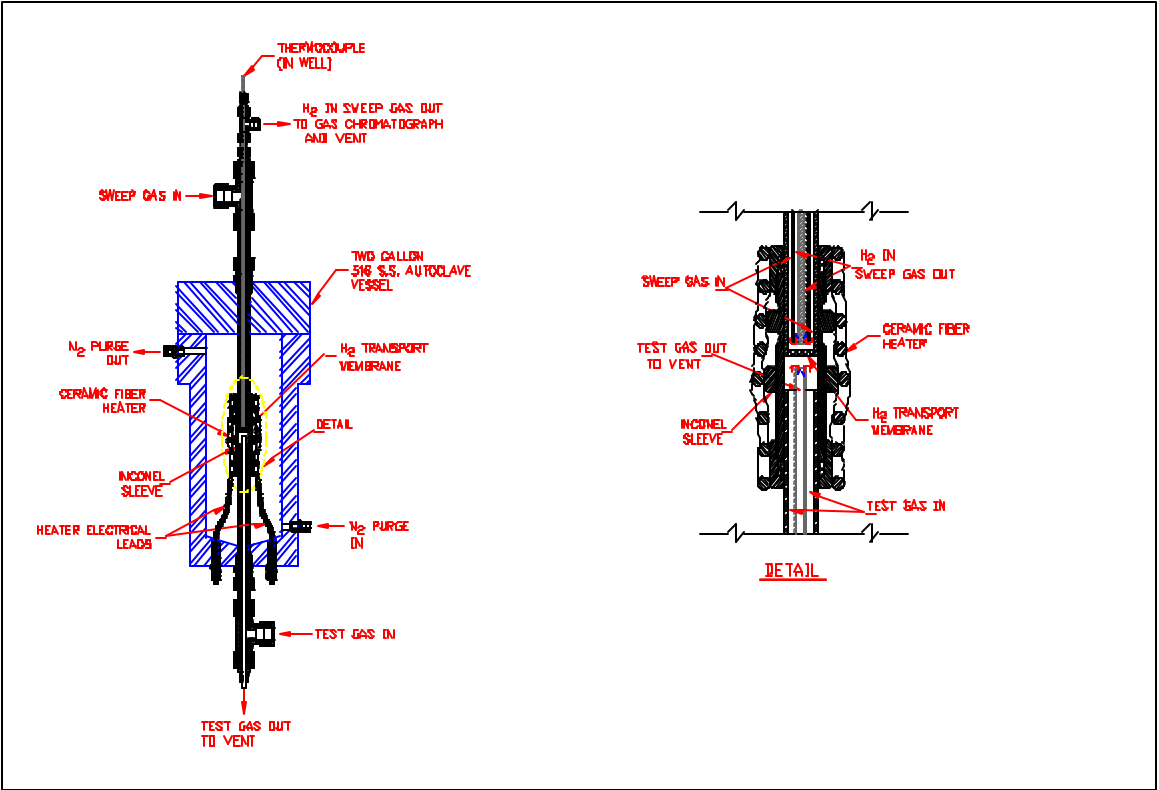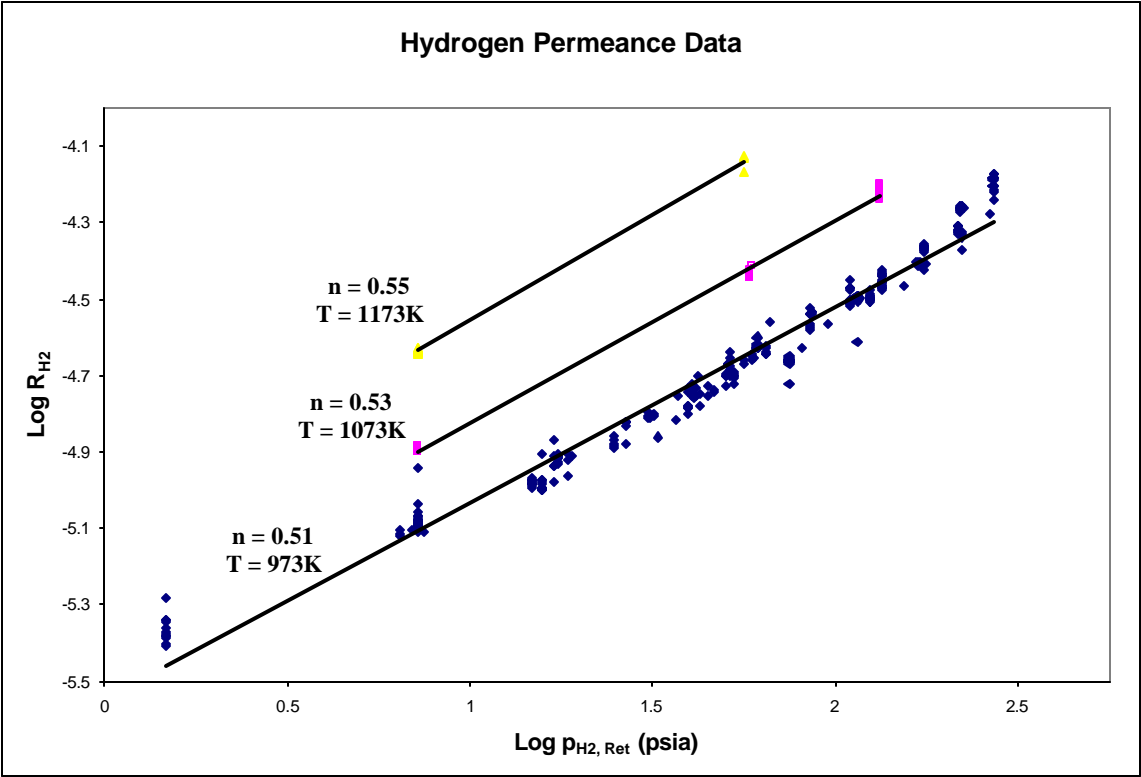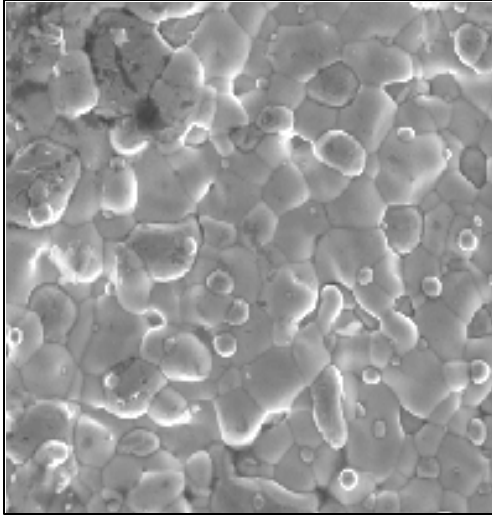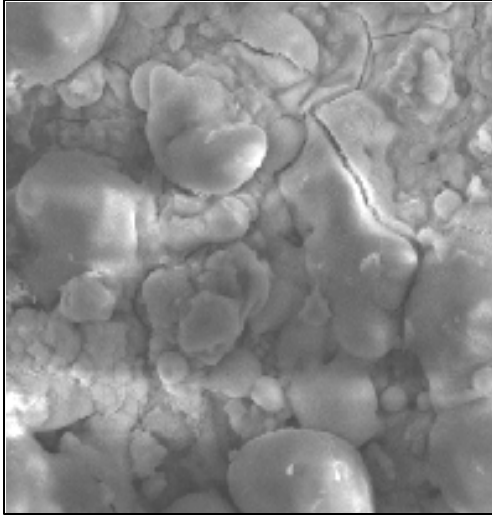
Figure 1. Schematic of membrane reactor and detail of membrane mounting.
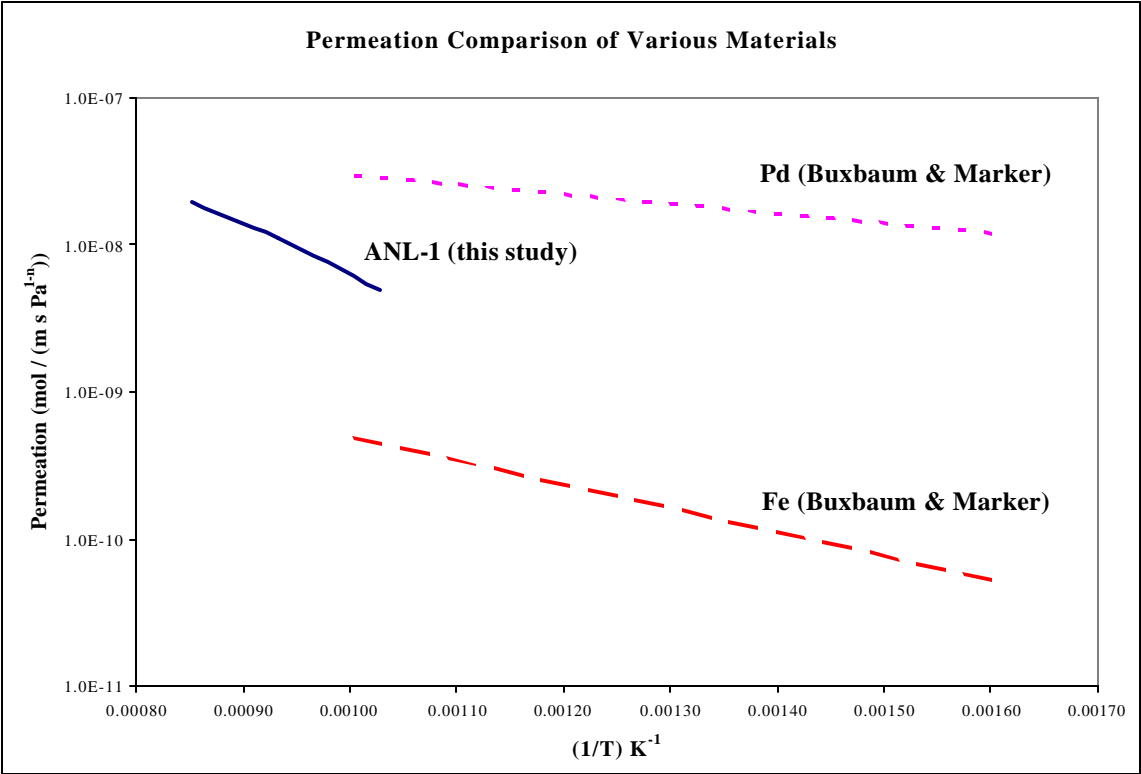
Figure 2. Hydrogen permeation data as a function of hydrogen partial pressure.
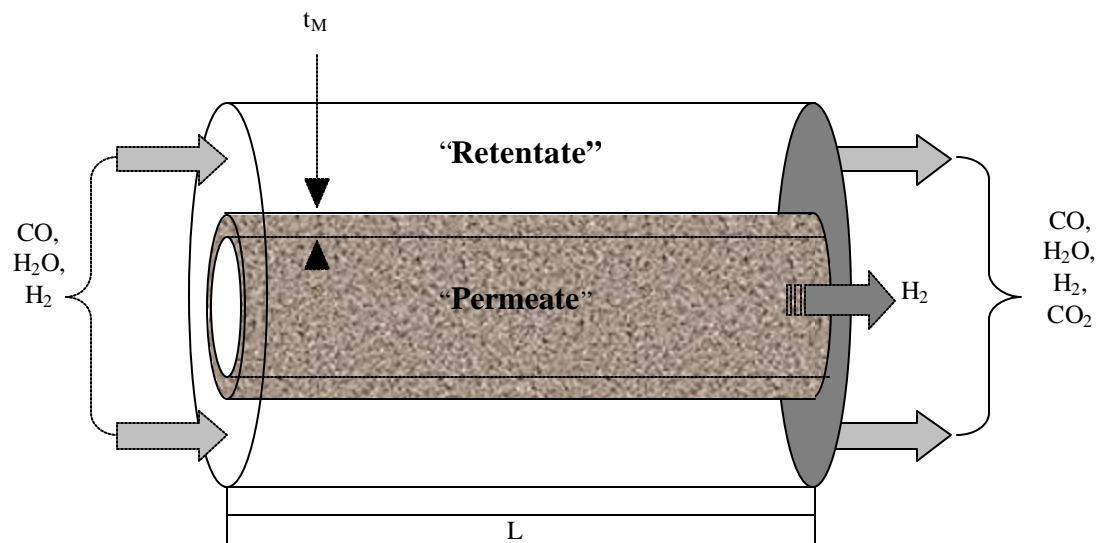
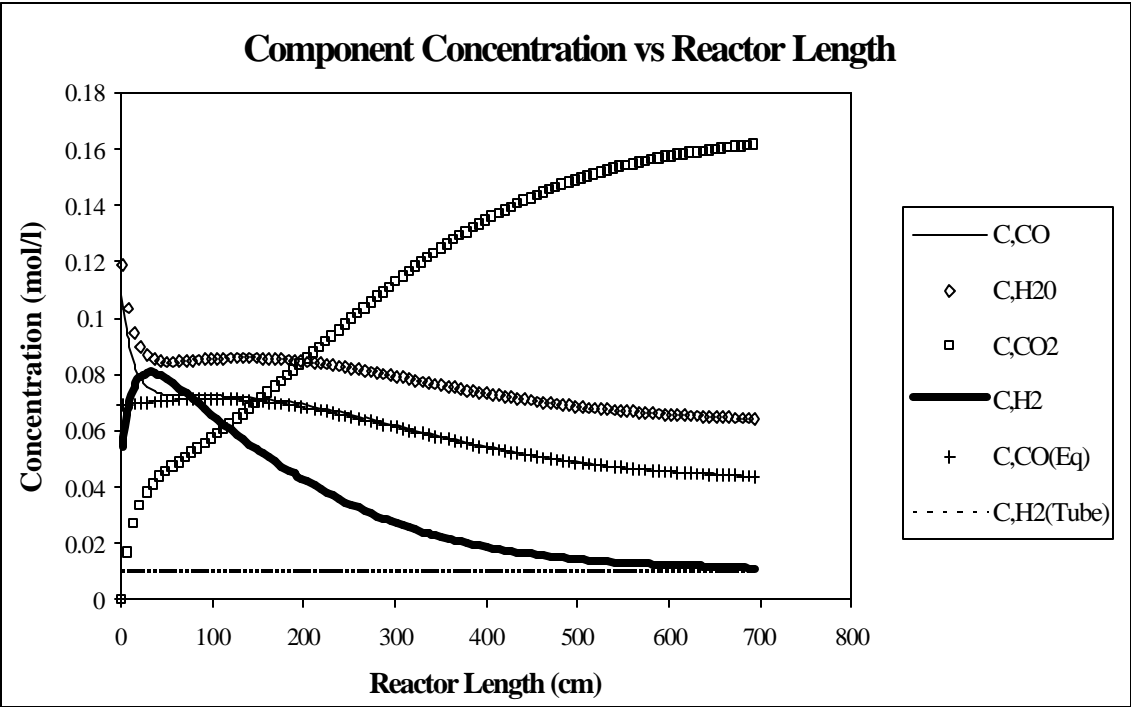**Figure 3a**. Pre-run membrane SEM photomicrograph (Magnification 2K).

Figure 3b. Post-run membrane SEM photomicrograph (Magnification 2K).

Figure 4. Comparison of permeability of ANL membrane to Pd and Fe as a function of temperature.

Figure 5. Schematic of reactor as modeled.

Figure 6. Component concentration as a function of reactor length for Water-Gas Shift modeling.
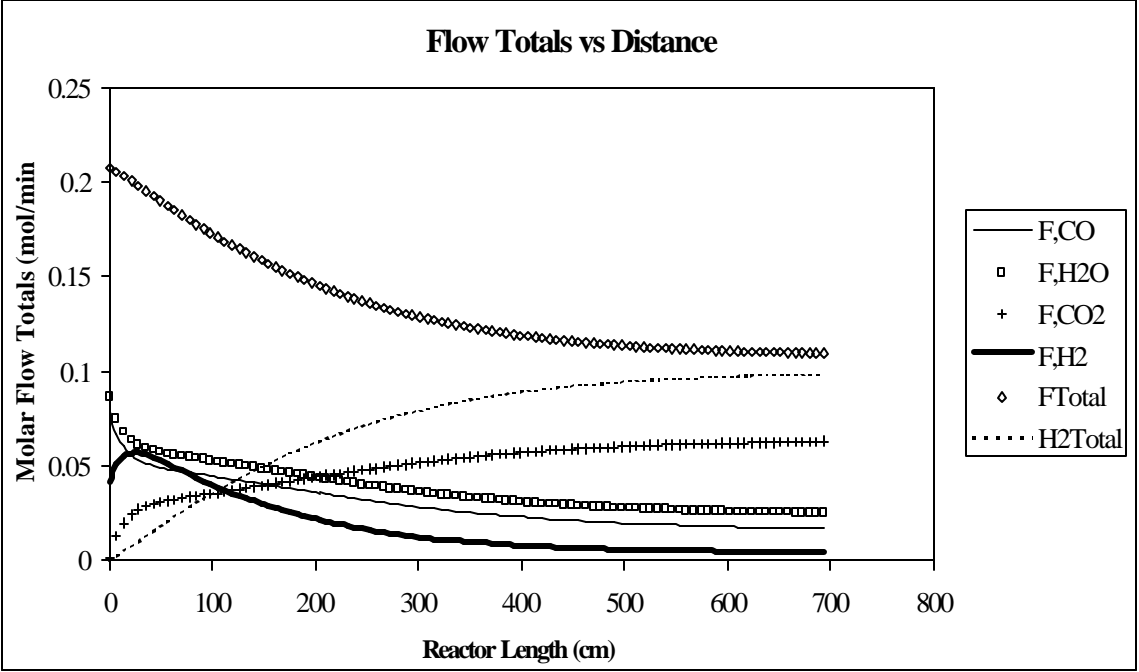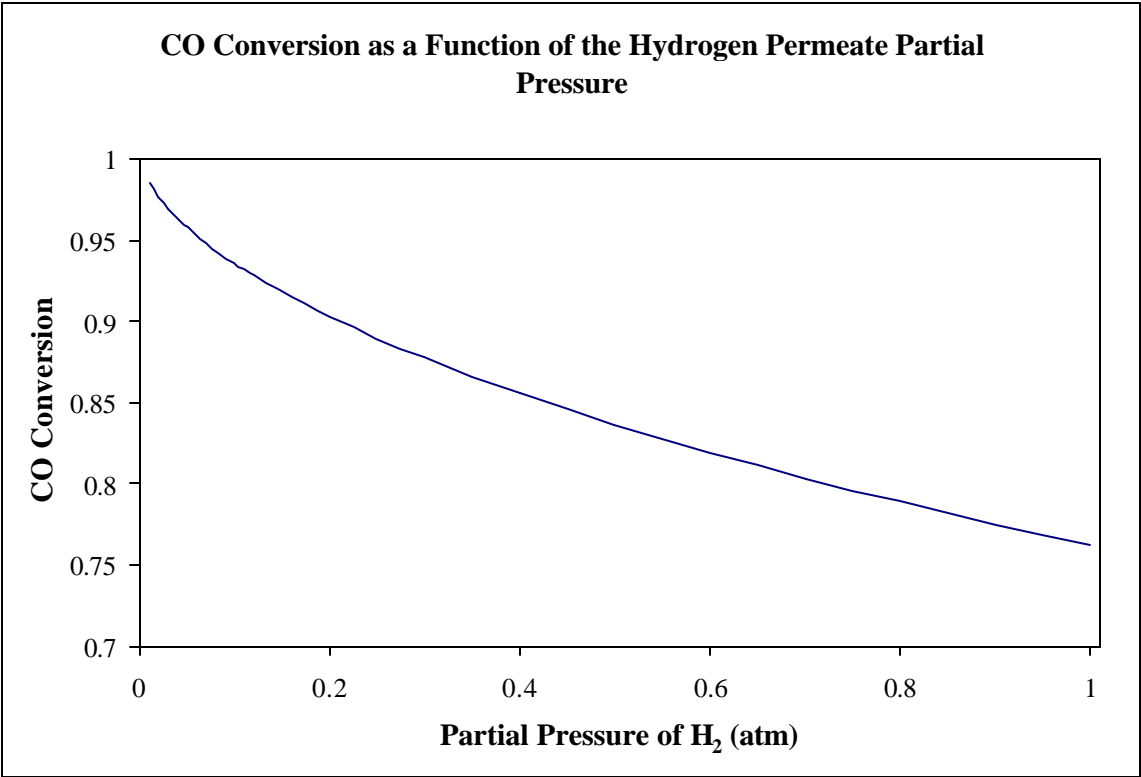
Figure 7. Flow totals as a function of reactor length for Water-Gas Shift modeling.

Figure 8. CO conversion as a function of the H_2 permeate partial pressure for Water-Gas Shift modeling.